

Hans Peter Kleiber · Frank Niessen

Variations of continental discharge pattern in space and time: implications from the Laptev Sea continental margin, Arctic Siberia

Received: 16 October 1999 / Accepted: 10 July 2000 / Published online: 7 November 2000
© Springer-Verlag 2000

Abstract Variations in sediment input and distribution to the Laptev Sea continental margin during the Holocene and Termination I could be identified based on radiocarbon dated magnetic susceptibility logs and sediment thickness in high-resolution seismic profiles. Magnetic susceptibility of surface samples reveals an increased input of magnetic grains to the Laptev Sea deriving from the Anabar and Khatanga river catchments. Exposed magnetite schists and volcanic rocks of the Anabar shield and Putoran Plateau, respectively, function as major source of magnetic material. The distribution of magnetic susceptibility in association with the thickness of the Holocene sediments indicates bottom-current induced sediment transport guided by major submarine valleys on the Laptev Sea shelf. The sites of filled paleoriver channels identified in the seismic profiles suggest that during the Late Weichselian sea-level lowstand river runoff continued through four of the major valleys on the exposed Laptev Sea shelf. The sediments at the top of the lowstand deposits in front of the Anabar-Khatanga valley, represented in the seismic profiles by prograding deltas, are characterized by outstandingly high magnetic susceptibility values. Radiocarbon datings approximate the deposition of these high magnetic sediments between 10 and 13.4 ka. It is suggested that this increased input of magnetic material is related to the deglaciation of the Anabar shield and the Putoran Plateau and thus support their glaciation during marine isotope stage (MIS) 2.

Keywords Laptev Sea · Arctic Ocean · Late Weichselian · Holocene River discharge · Magnetic susceptibility · High-resolution seismic

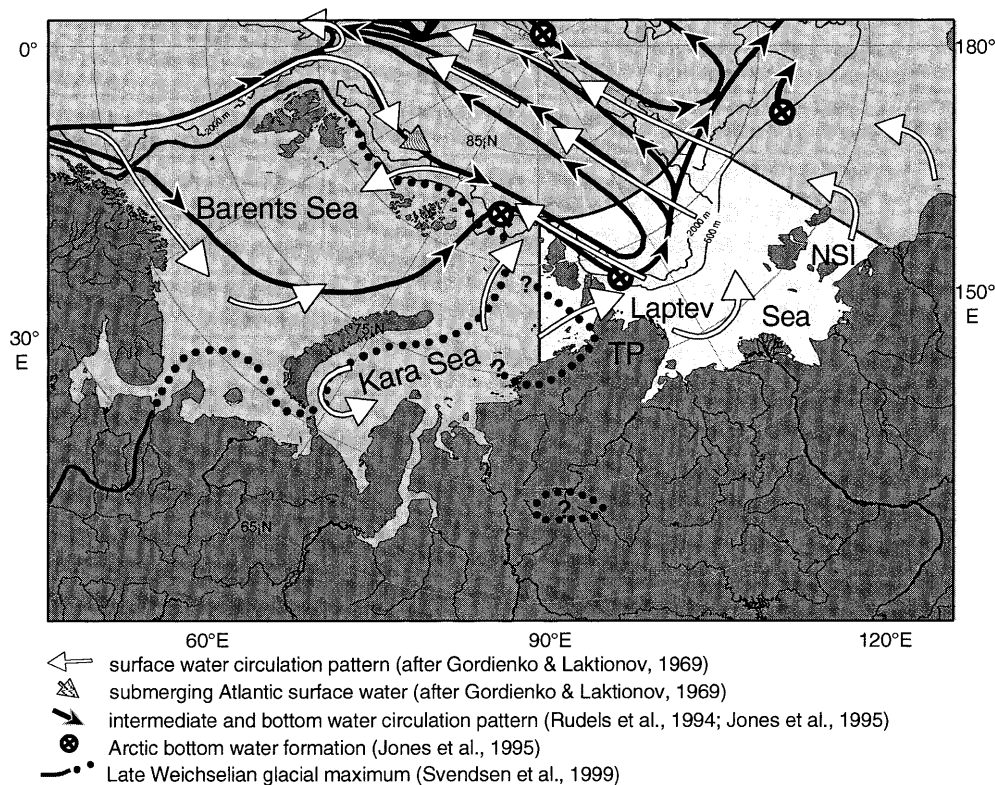
Introduction

Sedimentation in the Eurasian part of the Arctic Ocean is dominated by high inputs of terrigenous material derived from the surrounding land masses, supplied by major river systems and coastal erosion (Are 1994; Rachold et al. 1997). Biological productivity is relatively low compared with other oceans because of the permanent sea-ice cover (Stein 1996). Therefore, the distribution pattern of mineralogical parameters in space and time can be used to study the imprint of processes on the sedimentary record and to document past changes in the depositional environment (e.g., Wahsner et al. 1999, and references therein).

In marine sediments magnetic susceptibility is routinely measured on whole sediment cores and is often used for high-resolution lateral core correlation (e.g., Nürnberg et al. 1995; Stein et al. 1999, in press; Stein and Fahl 2000). Magnetic susceptibility is defined as the dimensionless proportional factor of an applied magnetic field in relation to the magnetization in the sample (expressed in SI units). On the basis of frequency-dependent magnetic susceptibility measurements a significant in situ formation of ultrafine (<0.03 mm) superparamagnetic, ferrimagnetic minerals produced by bacteria and chemical processes (e.g., Chang and Kirschvink 1989; Thompson and Oldfield 1986; Dearing 1994) as well as aeolian input can be excluded in the sediments of the Eurasian part of the Arctic Ocean (Niessen and Weiel 1996). Variations in magnetic susceptibility in sediments of the Eurasian part of the Arctic Ocean therefore exhibit changes of input of ferrimagnetic grains (magnetite, titanomagnetite or maghemite; Thompson and Oldfield 1986) derived from terrestrial bedrock erosion. Volcanic rocks can contain significantly higher amounts of ferrimagnetic minerals than other rock types. Consequently, magnetic susceptibility can be used to dis-

H. P. Kleiber · F. Niessen (✉)
Alfred Wegener Institute for Polar and Marine Research,
Columbusstrasse, Postfach 120161, 27515 Bremerhaven,
Germany
E-mail: fniessen@awi-bremerhaven.de

Fig. 1 Regional setting of the study area (brighter area) at the Central Siberia continental margin. The bathymetry is shown by the 500- and 2000-m contours. The surface water circulation is represented by *white arrows* (after Gordienko and Laktionov 1969); the intermediate and bottom circulation pattern are represented by *black arrows* (after Rudels et al. 1994; Jones et al. 1995). The *dotted line* shows the maximum extend of the Late Weichselian glaciation according to the hypothesis of Svendsen et al. (1999). *TP* Taymyr Peninsula; *NSI* New Siberian Islands



tinguish different source areas of terrigenous sediments in the ocean sediments and transport pathways can be identified (Thompson and Oldfield 1986).

High-resolution seismic profiles (Parasound, 4 kHz), radiocarbon-dated sediments and the sequence stratigraphic concept (e.g., Emery and Myers 1996) led Kleiber et al. (in press) to suggest that during the Late-Weichselian sea-level lowstand continuous river runoff across the exposed Laptev Sea shelf led to the formation of river deltas along the western Laptev Sea shelf edge. The deltas are covered by a thin drape of Holocene sediments. These sediments were deposited mainly during the early Holocene transgression of the Laptev Sea Area, which was not covered by an ice sheet from marine isotope stage (MIS) 3 to MIS 1.

In this study we present maps of the magnetic susceptibility distribution of surface samples, the top sediment layer of the Late-Weichselian sea-level lowstand deltas, the sediment thickness of the Holocene deposits, and the sea-level lowstand deltas. Our aim is to identify sediment source areas, to document variations in the depositional environment, and to reconstruct the sediment pathways to the continental margin of the Laptev Sea (Fig. 1) during these two time intervals.

Materials and methods

The investigated sediment cores were collected during the RV "Polarstern" cruises ARK-IX/4 (Fütterer

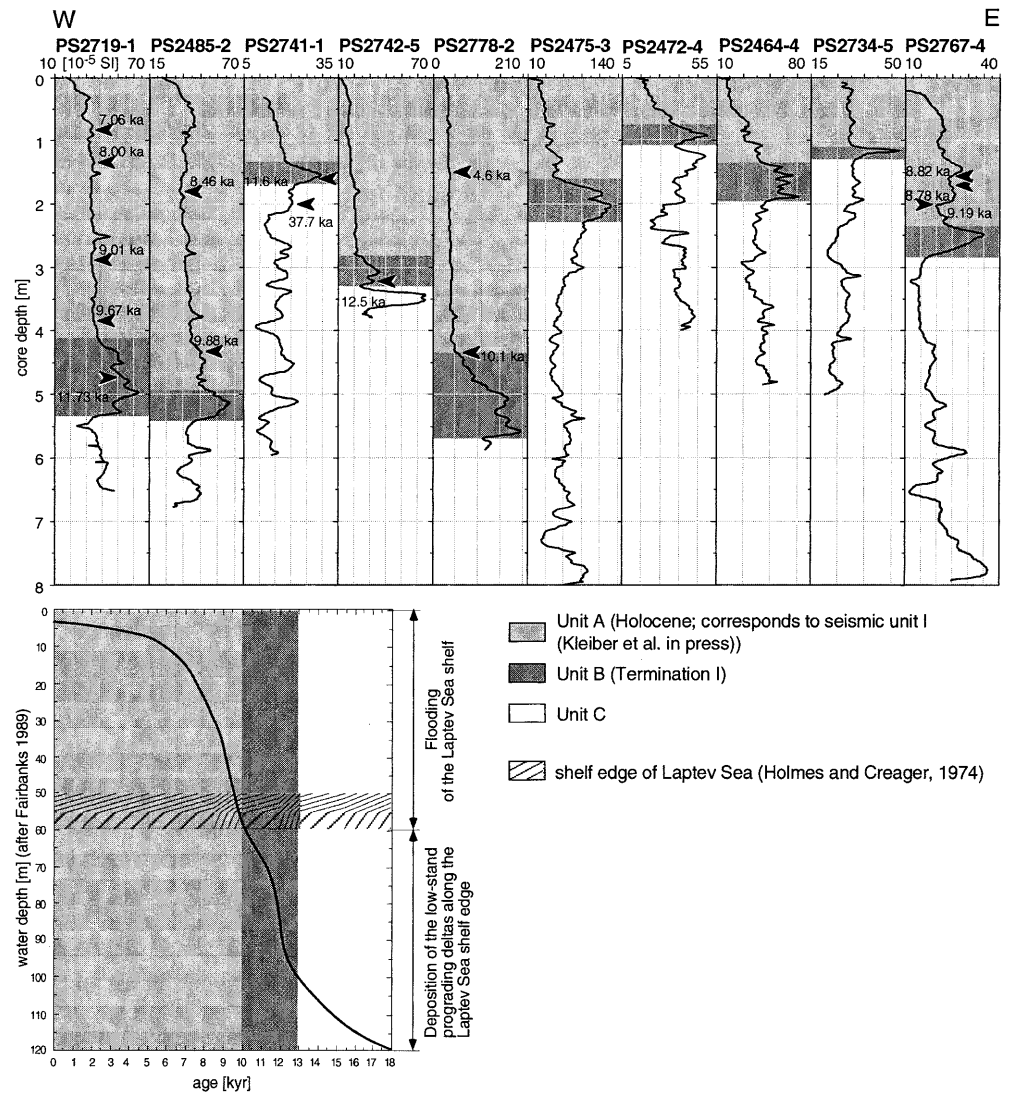
1994), ARK-XI/1 (Rachor 1997), and ARK-XIV 1-B, using a gravity (12-cm core diameter) and Kastenlot corer (rectangular cross section of 30×30 cm; Kögler 1963).

The volume magnetic susceptibility is routinely determined on board at 1- to 2-cm intervals on entire core sections, using a Bartington MS-2 loop sensor (Fig. 2). Measurements (10^{-5} SI) are corrected by a sensor-specific correction factor, according to the manual of the Bartington MS2B sensor system (For specifications see Table 1). Samples collected during the cruise Transdrift I (RV "Ivan Kireyev"; Kassens and Karpiv 1994) are included in the distribution map of the magnetic surface susceptibility (Fig. 3). The volume magnetic susceptibility of these freeze-dried sur-

Table 1 Bartington MS-2 loop sensor specifications used during the different cruises

	ARK-IX/4	ARK-XI/1 and ARK XIV 1-B
Loop sensor type	MS-2B (Bartington Ltd.)	
Loop sensor diameter	14.5 cm	14 cm
Coil diameter (D_c)	15.3 cm	14.8 cm
Core diameter (d) SL	12 cm	
Core diameter (d) KAL	98.36 cm	
Alternating field frequency	Approximately 80 A/m RMS	
Magnetic field intensity	0.565 kHz	
Loop sensor correction coefficient	$-0.0401777814 + 2.58316811 + (d/D_c)^{2.26972891}$	
Measurement interval	2 cm	1 cm
Measuring time	10 s	

Fig. 2 Magnetic susceptibility logs of cores from the Laptev Sea continental margin and eastern Kara Sea (for locations and water depth see Fig. 4). The estimated uniform Holocene deposits are *light-gray shaded*, whereas the distinct peak, representing Termination-I deposits, are *dark-gray shaded*. The lower sketch shows the deposition of the two units in relation to the global sea-level curve of Fairbanks (1989) and the water depth of Laptev Sea shelf edge after Holmes and Creager (1974). For reference of AMS ^{14}C datings see Table 2



face samples (13.6 cm^3) were measured by Niessen and Weiel (1996) at high (4.6 kHz) and low (0.46 kHz) frequencies in SI units (10^{-5}) using a MS2B Bartington (UK) susceptibility control unit. The volume magnetic susceptibility of defined sample volumes (13.6 cm^3) measured by the MS2B Bartington susceptibility control unit can be directly compared with the corrected loop sensor measurements (M. Pirrung, pers. commun.).

High-resolution sub-bottom profiles were recorded by the hull-mounted Parasound echosounder (4 kHz; cf. Grant and Schreiber 1990 for technical details). A seismic velocity of 1500 m/s was used to estimate sediment thickness.

The evaluated seismic profiles recorded during RV "Polarstern" cruises ARK-IX/4 (Fütterer 1994), ARK-XI/1 (Rachor 1997), and ARK-XIV 1-B are used to determine the thickness of the uppermost two seismic units. The different echo characters are classified after the schemes of Damuth (1975, 1980) and Pratson and Laine (1989).

Results

The magnetic susceptibility logs of the cores from the study area can be subdivided into three characteristic units, named A (youngest) to C (Fig. 2). Unit A shows low, uniform magnetic susceptibility values, varying between 10 and 60×10^{-5} SI with a generally decreasing trend of amplitudes from shallower to deeper water (Fig. 2). Radiocarbon dates (Fig. 2; Table 2) from unit A span from 9.88 to 4.6 ka indicating a Holocene age, with the base of the unit having an age close to 10 ka. The transition to the underlying unit B is marked by a distinct increase in magnetic susceptibility (Fig. 2). Unit B is characterized by magnetic susceptibility peak values, which are used for lateral core correlations (Fig. 2; cf. Stein et al., in press). Peak values range from 35×10^{-5} SI northeast of Severnaya Zemlya up to 200×10^{-5} SI in core site PS2778, situated at the shelf edge of the western Laptev Sea (Fig. 2, 4). The estimated Holocene boundary at the base of unit A,

Fig. 3 The magnetic susceptibility distribution of the surface samples on the Laptev Sea continental margin. The arrows reveal the general surface circulation pattern and river input (modified after Suslov 1961)

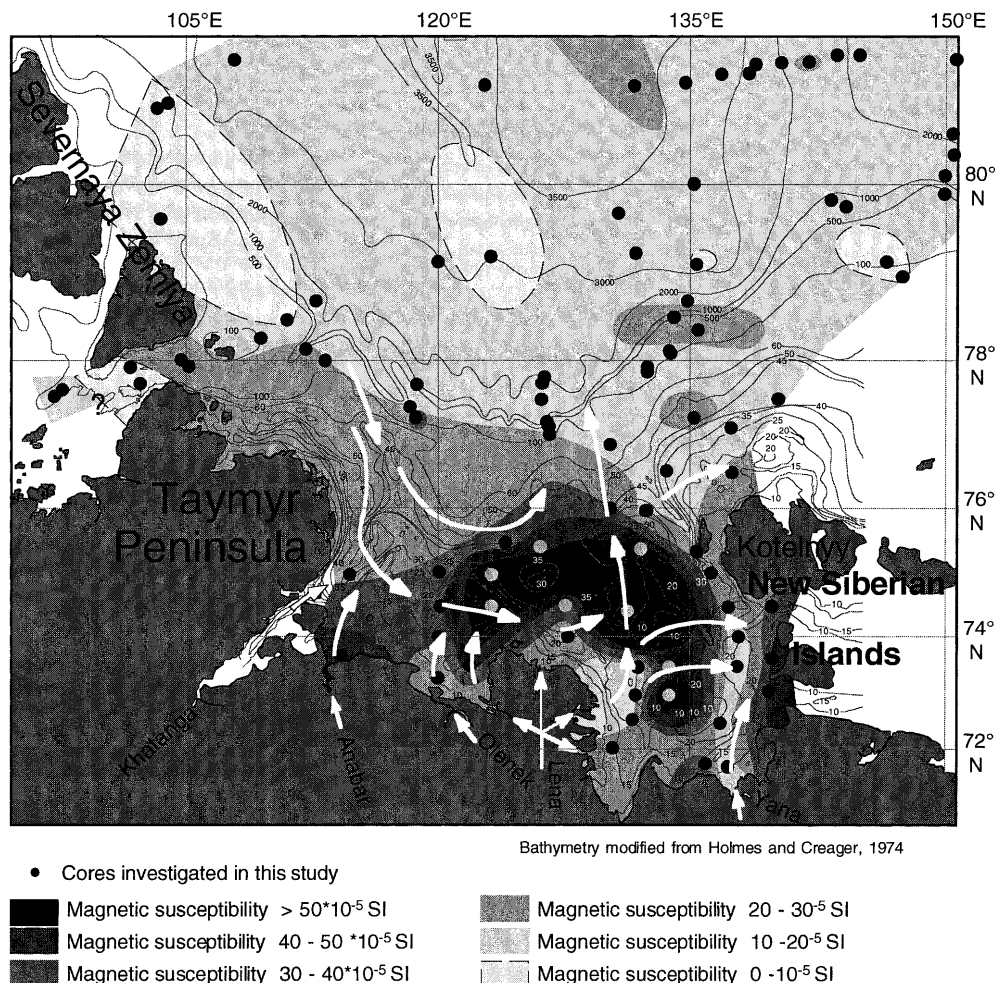


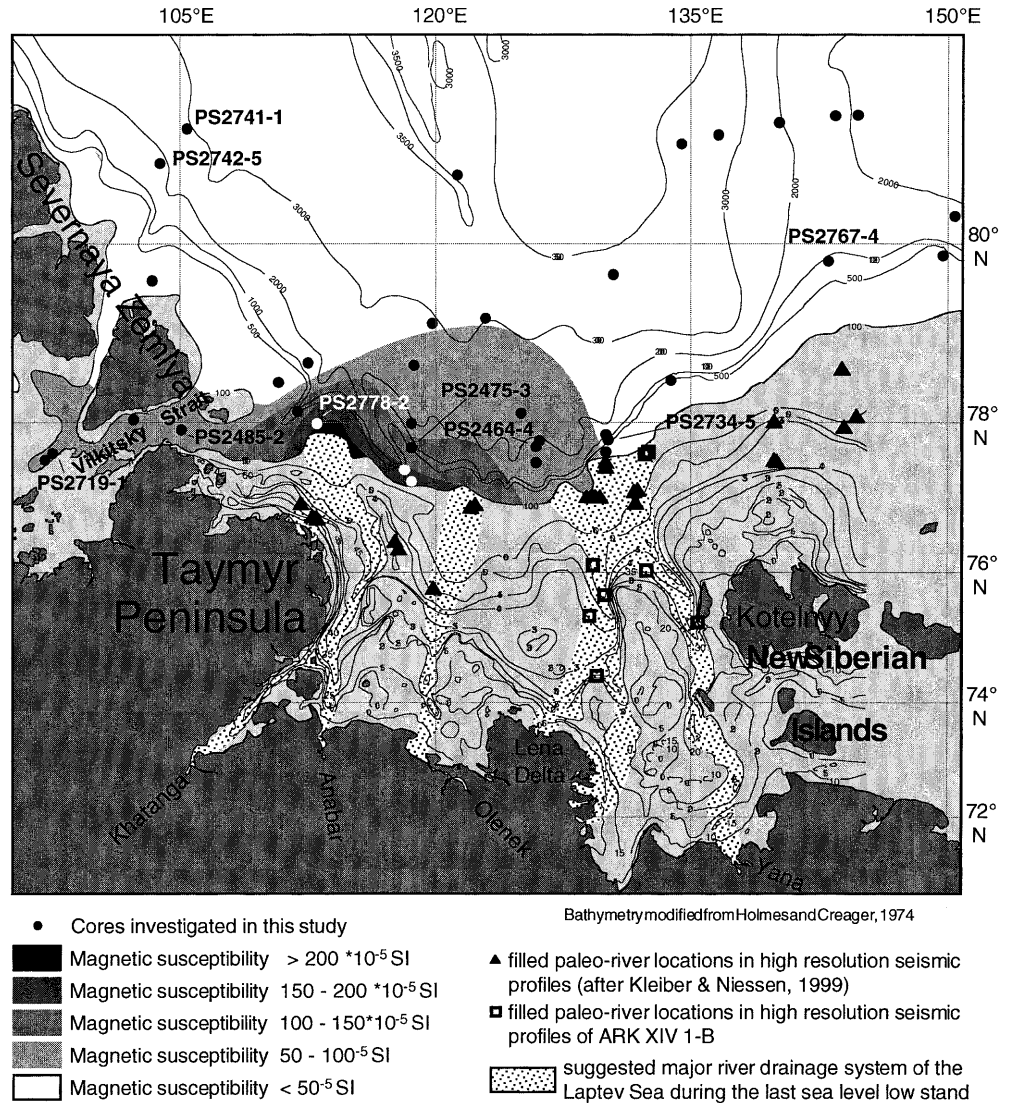
Table 2 Results of accelerator mass spectrometry (AMS) ^{14}C dates performed on bivalves, *N. pachy sin.* and mixed foraminifers at the Leibniz Laboratory for Radiometric Dating and Stable Isotope Research, University of Kiel, Germany

Core	Sample no.	Depth (cmbsf)	Carbon source	^{14}C Age (B.P.)	Reservoir effect (B.P.)	^{14}C Age (corr., B.P.)	Reference
PS2485-2	KIA112	180	Bivalves	8900	-440	8460±60	Weiel (1997)
PS2485-2	KIA113	435	Bivalves	10320	-440	9880±80	
PS2719-1	KIA8212	84	Bivalves	7500	-440	7060±35	Stein et al.
PS2719-1	KIA8213	136	Bivalves	8435	-440	7995±40	(in press)
PS2719-1	KIA8214	289	Bivalves	9450	-440	9010±55	
PS2719-1	KIA8215	385	Bivalves	10105	-440	9665±50/-45	
PS2719-1	KIA8216	473	Bivalves	12165	-440	11725±60	
PS2741-1	KIA4764	160	Mixed forams	12040	-440	11600±70	Knies et al. (1999)
PS2741-1	KIA110	200	<i>N. pachy sin.</i>	38160	-440	37720±3500/-2500	
PS2742-5	KIA2737	324	Mixed forams	12910	-440	12470±80	Knies (1999)
PS2767-4	KIA1471	152-154	Bivalves	9260±40	-440	8820±40	R.F. Spielhagen
PS2767-4	KIA1472	172-174	Bivalves	9220±40	-440	8780±40	(unpublished data)
PS2767-4	KIA1473	200-202	Bivalves	9630±40	-440	9190±40	
PS2778-2	KIA119	153	Bivalves	5040	-440	4600±60	Weiel (1997)
PS2778-2	KIA120	434	Bivalves	10510	-440	10070±60	

and radiocarbon datings in cores PS2719-1, PS2741-1, and PS2742-5 (Fig. 2), give mean linear sedimentation rates (LSR) for unit B of approximately 35.8, 21.6, and 17.0 cm/ky, respectively. These LSR are comparable to mean Holocene LSR along the Laptev Sea continental margin (e.g., Bauch et al. 1996; Spielhagen et

al. 1996; Weiel 1997; Stein et al. 1999, in press; Stein and Fahl 2000). On basis of the estimated Holocene boundary and the LSR, the initial deposition of unit B was extrapolated in cores PS2719-1, PS2741-1, and PS2742-5 to 13.4, 12.5, and 12.8 ka, respectively. The transition to unit C is represented by a distinct

Fig. 4 The magnetic susceptibility distribution of the distinct peak representing the top of seismic unit II. *Light-gray shading* represents the exposed shelf area (~ 100 m) during the Late Weichselian sea-level lowstand. The *dotted areas* on the exposed Laptev Sea shelf, represent the courses of the major rivers draining directly to the shelf edge



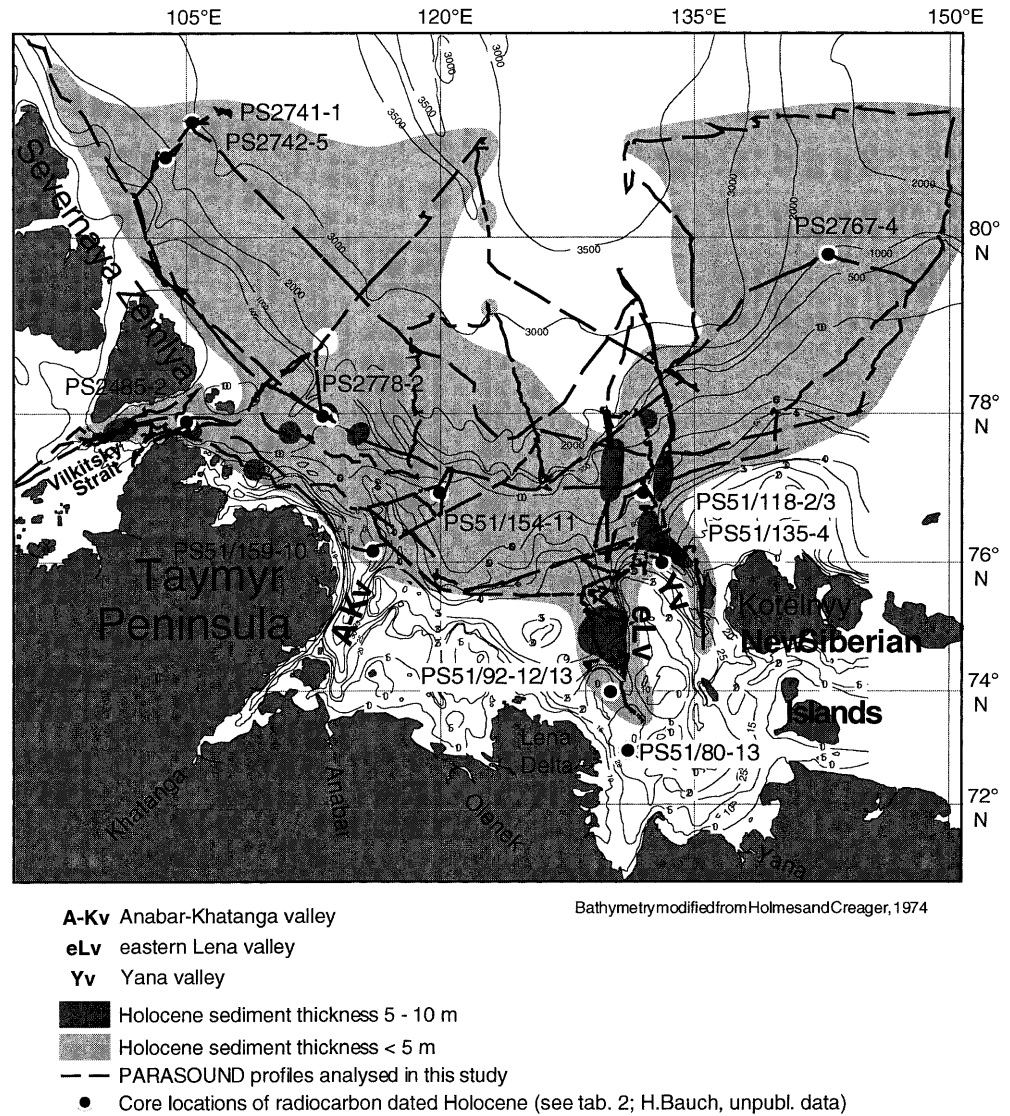
decrease in magnetic susceptibility. The magnetic susceptibility values of unit C range from $10 \cdot 10^{-5}$ SI in core PS2741-1 northeast of Severnaya Zemlya up to $90 \cdot 10^{-5}$ SI in core PS2475-3 on the western Laptev Sea continental margin (Figs. 2, 4). The magnetic susceptibility values of unit C are more variable than those of unit A (Fig. 2).

The distribution pattern of the surface samples (Fig. 3) reveals that the highest values are determined in the central Laptev Sea. Increasing values are measured toward the estuary of the Anabar river and south of Koteln'y. The lowest magnetic susceptibility values are recorded in front of the estuaries of the Lena and Yana rivers. North of the Yana river estuary, following the Yana submarine valley (Holmes and Creager 1974), the surface sediments show low magnetic susceptibility values (Fig. 3). From the Laptev Sea continental slope down to the abyssal plain, the magnetic susceptibility values generally range between 10 – $20 \cdot 10^{-5}$ SI, with patches of slightly higher or lower values (Fig. 3).

Using the peak values of unit B, the lateral distribution of the magnetic susceptibility in this marker horizon shows an almost concentric decrease north of core PS2778-2 (Fig. 4). Strong gradients occur toward the northern and northwestern Laptev Sea continental rise, whereas the decrease of magnetic susceptibility towards the Vilkitsky Strait and northeastern Laptev Sea continental margin is more gradual (Fig. 4).

In the Parasound profiles of the upper sedimentary succession of the western Laptev Sea continental slope and rise, four seismic units, I (youngest) to IV, have been identified (Kleiber et al., in press). The base of seismic unit I has been identified in Parasound profiles from almost the entire Laptev Sea continental margin by a medium- to high-amplitude seismic reflector and the mapped area could thus be expanded in this study (Fig. 5). Unit I forms an acoustically transparent drape across the entire area (Fig. 6). In general, the Parasound profiles show that the thickness of the Holocene deposits varies between 1 and < 5 m (Fig. 5), resulting in an LSR between 10–50 cm/ky. The thick-

Fig. 5 The thickness of the Holocene deposits, estimated according to the thickness of the uppermost seismic unit in the Parasound profiles, shown as *dotted black lines*. In the shown core sites, the thickness of the Holocene sediments could be verified based on radiocarbon datings (see Table 2 and H. Bauch, unpublished data)



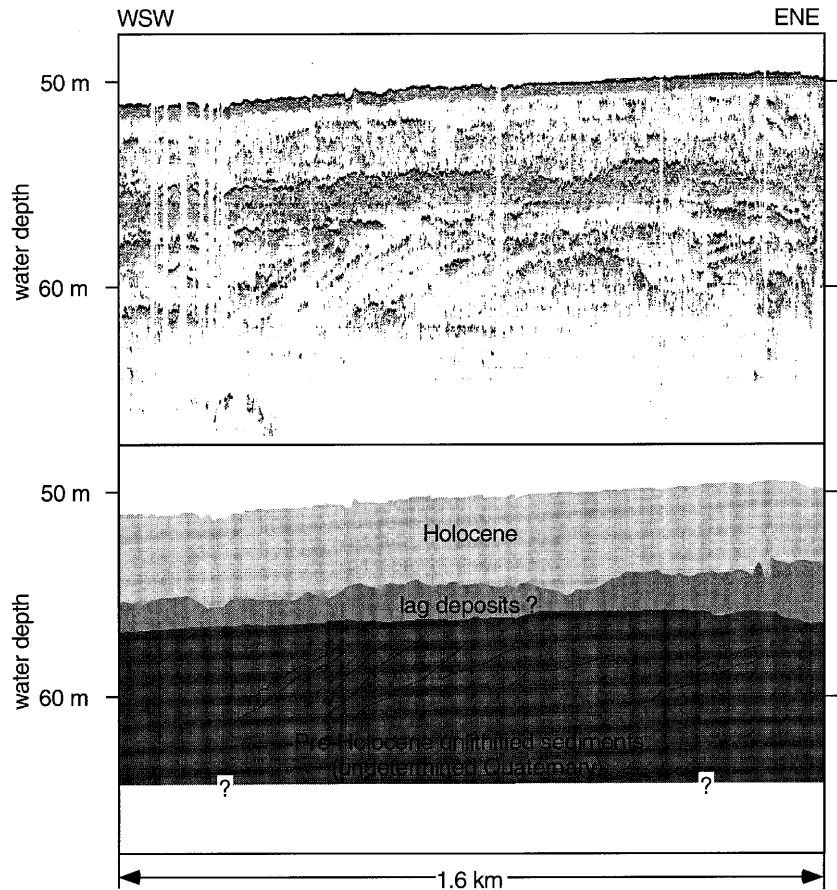
ness of seismic unit I is seen to reach up to 10 m and to show a layered internal reflection pattern only in few profile sections (Fig. 7). These high accumulation depocenters are situated in the western Vilkitsky Strait, north of Taymyr Peninsula, at the shelf edge north of the Anabar-Khatanga submarine valley, in the southern part of the eastern Lena submarine valley, and in the northern section and on the shelf north of the Yana submarine valley (Fig. 5). On the Laptev Sea shelf, seismic unit I is often bounded by a continuous, distinct to prolonged basal reflector. The acoustic penetration is limited to <10 m, and no reflectors are recorded from below the prolonged basal reflector. The thickness of seismic unit I correlates with the thicknesses of the uniform upper core sections (Fig. 7); therefore, we support the suggestion by Kleiber et al. (in press) that seismic unit I represents mainly Holocene deposits.

Eight channels were identified and mapped in addition to the 24 filled paleoriver channels identified by

Kleiber and Niessen (1999) based on their erosive, U-shaped sub-bottom morphology and undeformed fill geometry (Fig. 4). The filled paleoriver channels are up to 11 m deep. They are covered by the uppermost seismic unit and situated in the eastern Lena and Yana submarine valleys (Fig. 4).

Parasound profiles from the Laptev Sea continental slope and rise reveal that unit B of the cores represents the top of seismic unit II (Fig. 7). Along the western Laptev Sea shelf edge, this second seismic unit is characterized by prograding wedges up to 100 m thick (Fig. 8). Kleiber et al. (in press) interpret these prograding wedges as lowstand deltas, deposited during the Late Weichselian sea-level lowstand (MIS 2). On the Laptev Sea shelf, the second seismic unit is not present.

Fig. 6 Parasound profile of the northern, eastern Lena valley (*eLv*; see Fig. 5) between 75°45'N/130°24'E and 77°46'N/130°27'E, showing the transparent upper seismic unit I, interpreted as Holocene deposit



Discussion

The distribution of the magnetic susceptibility in the surface sediments of the Laptev Sea suggests that the magnetic material is supplied by the Anabar and probably Khatanga rivers (Fig. 3). In the catchment area of the Anabar river, the magnetic material is derived from the magnetite schists exposed in the Anabar shield (Fig. 9; Vinogradov et al. 1973). This source region is also indicated in surface sediments of the western Laptev Sea by increased contents of pyroxene (Stein and Korolev 1994; Behrends 1999; Peregovich et al. 1999), which is derived from the pyroxene-plagioclase gneiss of the Anabar shield (Vinogradov et al. 1973). The Khatanga river drains a large area of Triassic volcanic rocks of the Putoran Plateau, including trappbasalts (Fig. 9; Duzhikov and Strunin 1992), which are a source of magnetite and titanomagnetite. In the surface sediments of the western Laptev Sea this source area is also indicated by the increased content of smectite (Wahsner et al. 1999). In contrast, the Paleozoic to Mesozoic sedimentary rocks in the catchment area of the Lena and Yana rivers do not contain large quantities of magnetic minerals. The magnetic susceptibility of the surface sediments in the eastern Laptev Sea is therefore low. The low magnetic surface

susceptibility from the estuary of the Yana river and along the Yana submarine valley to the north suggests that the drainage of the Laptev Sea is strongly controlled by the bathymetry. This concept is supported by the grain-size distribution of the surface sediments and the distribution of the main Holocene depocenters. The main Holocene depocenters are located in the eastern Lena submarine valley, in and north of the Yana submarine valley, and at the shelf edge north of the Anabar-Khatanga submarine valley (Fig. 5). The grain-size distribution implies that the deposition of silty clay, characterizing the fluvial input (Holmes and Creager 1974), is dominant in the Anabar-Khatanga, eastern Lena and Yana channels (Benthien 1994).

The increased magnetic susceptibility of the surface sediments south of Kotelnny and in the central Laptev Sea is significantly higher than the surface samples in front of the estuary of the Anabar river and indicates that other processes than pure riverine input have to be considered to explain the distribution pattern in these areas. The higher values south of Kotelnny may be related to the erosion of Paleozoic and Tertiary basalts and volcanic rocks exposed on the New Siberian Islands (Fujita and Cook 1990). Stein and Korolev (1994) also suggest that the high magnetite content in the surface sediments south of Kotelnny and in the

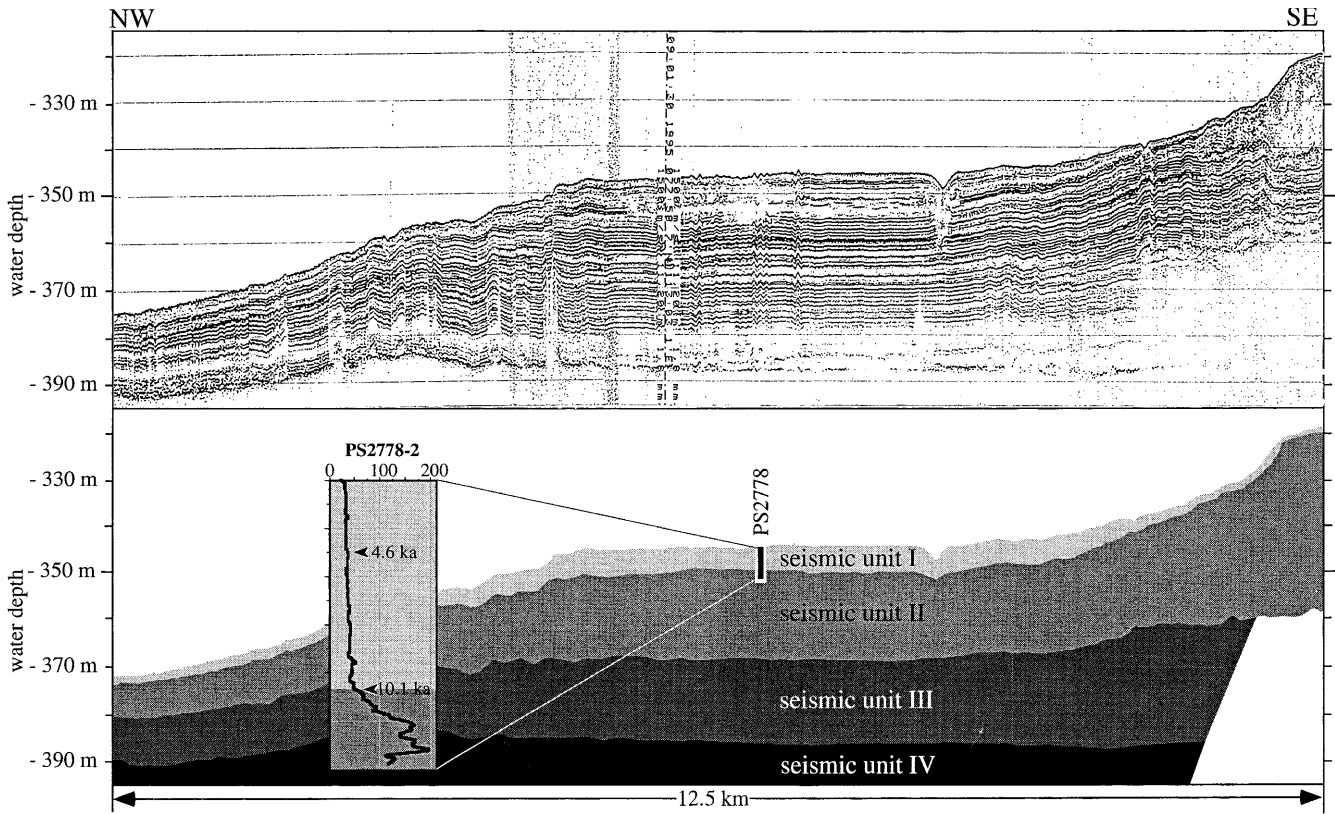


Fig. 7 Parasound profile shows a cross-section of the wedge-shaped deposits of seismic unit II in the site of core PS2778 at the western Laptev Sea continental shelf edge between

78°03'N/113°01'E and 77°57'N/113°16'E (for location see Fig. 4). Seismic units after Kleiber et al., in press

Fig. 8 The thickness of the prograding sea-level lowstand deltas along the western Laptev Sea shelf edge based on Parasound profiles

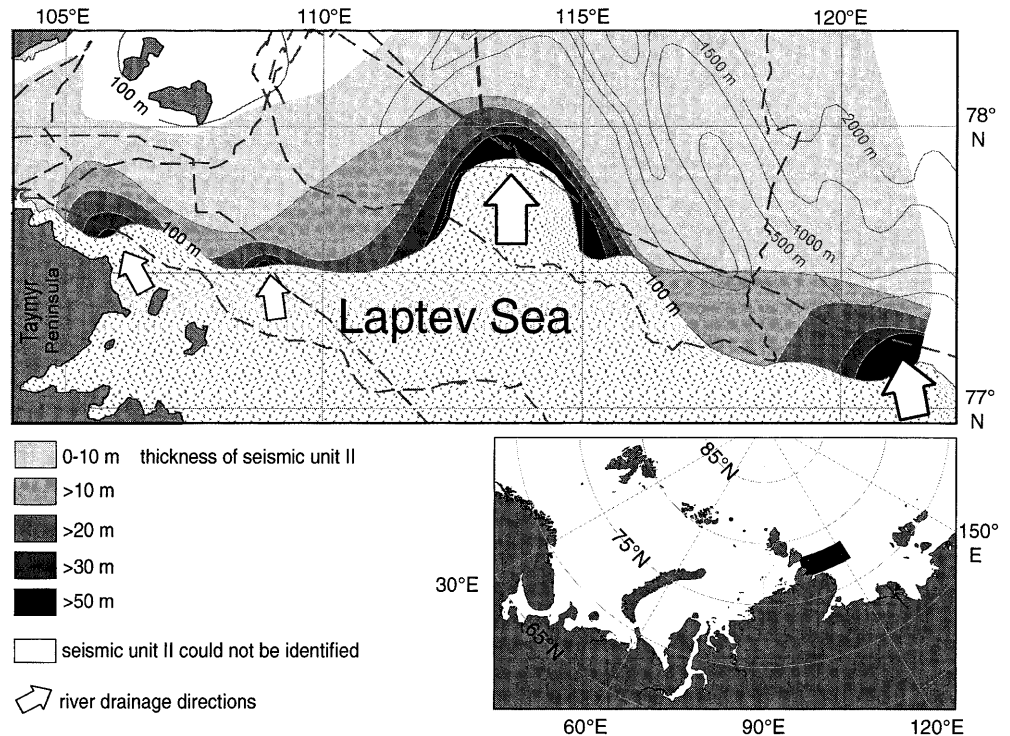
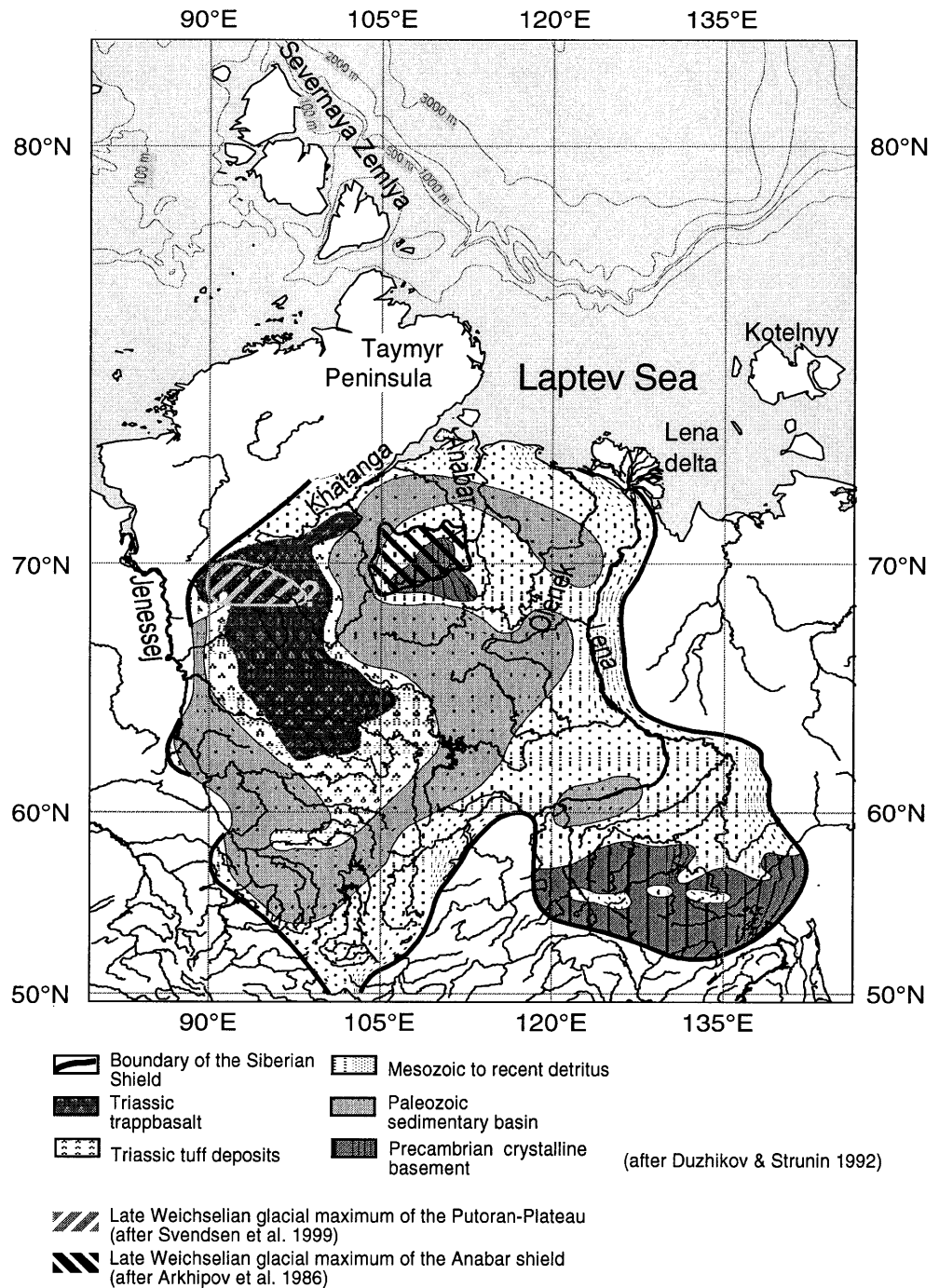


Fig. 9 Geological overview of the Noril'sk region. (After Duzhikov and Strunin 1992)

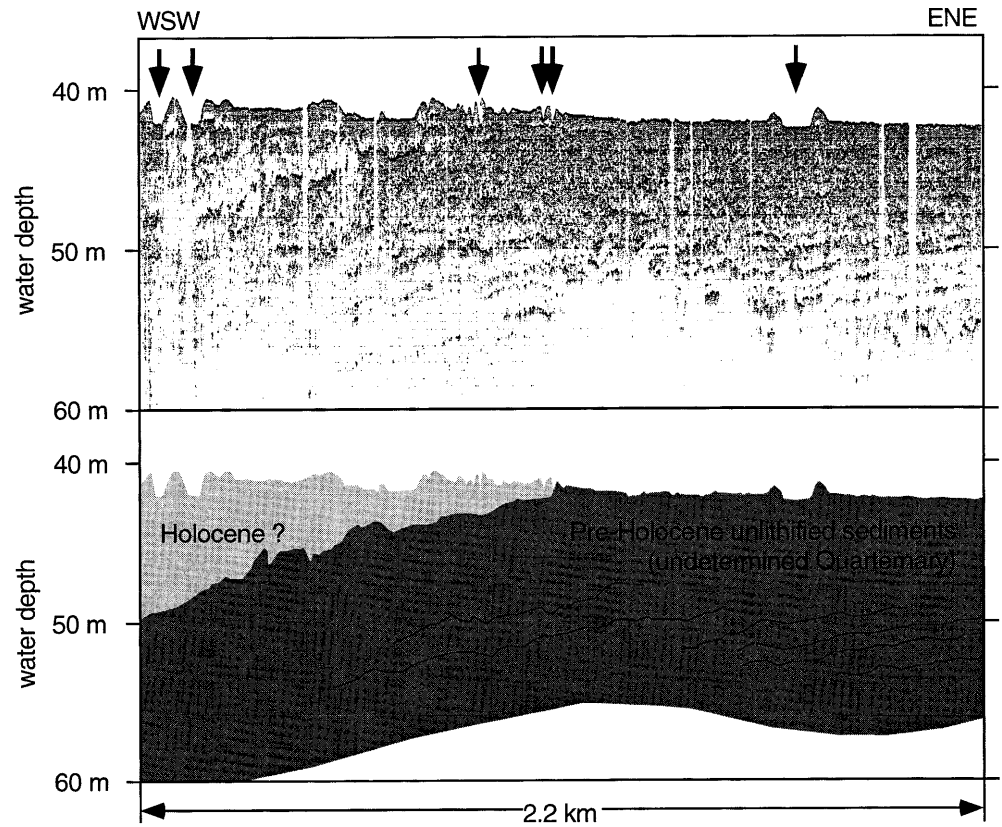


central part of the Laptev Sea may be due to erosional processes in these very shallow-water environments. Erosion, reworking, and redeposition of pre-Holocene sediments in the Laptev Sea are caused by wave-induced bottom currents (Are 1994) and ploughing by icebergs and sea-ice pressure ridges (Fig. 10). Examples of the latter are identified in the Parasound profiles from the northeast of the Taymyr Peninsula, the central Laptev Sea, and northwest of Kotelnyy (e.g., Rachor 1997).

On the Laptev Sea continental margin and in the eastern Kara Sea, radiocarbon datings reveal that the

deposition of the high magnetic material, indicated by characteristic peaks in the magnetic susceptibility logs, occurred approximately between 13.4 ka and the beginning of the Holocene (10 ka; Fig. 2; Stein and Fahl 2000; Stein et al., in press). In Parasound profiles from the western Laptev Sea, the high magnetic susceptibility deposits represent the top of lowstand deltas along the shelf edge, fed by point sources during MIS 2 (Kleiber et al., in press). During MIS 2, when the sea level was >100 m lower than at present (e.g., Blanchon and Shaw 1995; Fairbanks 1989; Shackleton 1987), the entire Laptev Sea was subaerially exposed.

Fig. 10 Parasound profile of the northeastern Laptev Sea between 76°25'N/133°32'E and 76°25'N/133°28'E shows exposed pre-Holocene sediments eroded by icebergs and sea-ice pressure ridges indicted by *black arrows*



Filled paleoriver channels in Parasound profiles (Fig. 4; Kleiber and Niessen 1999) and the bathymetry (Holmes and Creager 1974) lead us to suggest that the rivers remained active during MIS 2 and drained through four major valleys across the exposed Laptev Sea shelf (Fig. 4). A continuous river runoff during the last sea-level lowstand is also indicated by low planktonic $\delta^{18}\text{O}$ values in the central Arctic Ocean (Nürnberg et al. 1995; Nørgaard-Pedersen 1996).

Because of the proposed paleodrainage pattern (Fig. 4), we suggest that the two major prograding lowstand wedges at the western Laptev Sea shelf edge represent former deltas of the Anabar-Khatanga and Olenek rivers. The smaller deltas between 105° and 110°E (Fig. 8) are likely related to local drainage systems on the Taymyr Peninsula. These local drainage systems were according to the maximum extent of the Late Weichselian glaciation (Svendsen et al. 1999) not related to a local glaciation and subsequent drainage as proposed by Kleiber and Niessen (1999). The Anabar-Khatanga lowstand delta coincides spatially with the distribution of the highest magnetic susceptibility values in sediments deposited between approximately 13.4 and 10 ka along the western Laptev Sea continental margin (Fig. 4). Thus, during MIS 2 and Termination I, the Anabar-Khatanga paleoriver mouth acted as point-source for high amounts of magnetic minerals. The distribution of the magnetic susceptibility along the Laptev Sea continental margin (Fig. 4) likely reflects the Arctic Ocean circulation pattern during

Termination I, suggesting a west/east-oriented current parallel to the paleocoast. This implies that the circulation pattern during Termination I was comparable to the present intermediate and bottom-water circulation pattern (Fig. 1; Rudels et al. 1994; Jones et al. 1995). For this reason the higher magnetic susceptibility values in core PS2719-1 from the eastern Kara Sea (Figs. 2, 4) point to an increased input of magnetic material, probably from the Jenessej river, which drains the volcanic rocks of the western Putoran Plateau. The sediments in the top of the Anabar-Khatanga lowstand delta show LSR comparable to the Holocene sediments. The significantly higher magnetic susceptibility of the upper sediments of the Anabar-Khatanga lowstand delta (200×10^{-5} SI) compared with the surface values in the estuary of the Anabar river (45×10^{-5} SI) therefore indicate that the volcanic terrain of the Putoran Plateau and/or magnetite schists of the Anabar shield must have released considerably higher quantity of eroded material. We suggest that this increased input may reflect the deglaciation of the Putoran Plateau and/or Anabar shield. The peaks in the susceptibility logs date this deglaciation to the period from approximately 13.4 ka to approximately 10 ka (Termination I). The higher magnetic susceptibility values may therefore be used as an indicator for the mountain deglaciation of the Putoran Plateau as suggested by, for example, Velichko (1997), Melles et al. (1996), and the Anabar shield (Arkhipov 1995; Velichko et al. 1997).

Summary and conclusions

The surface distribution of the magnetic susceptibility in the Laptev Sea indicates that major source of magnetic material are the Anabar and Khatanga rivers. Magnetite schists exposed in the Anabar shield and extensive Triassic volcanic rocks, including trappbasalts, are suggested to be the main source areas. Low magnetic susceptibility values from the Yana estuary along the Yana submarine valley to the north, and the distribution of the thickest Holocene depocenters in or in front of the submarine valleys of the Laptev Sea shelf, indicate that the bottom circulation and related sediment transport is controlled by the bathymetry.

There is a distinct peak in the magnetic susceptibility logs from the cores of the western Laptev Sea continental slope and rise in the sediments deposited between approximately 13.4 and 10 ka. The distribution map of these magnetic susceptibility peak values reveals that the highest accumulation of magnetic minerals occurred in a sea-level lowstand delta in front of the Anabar-Khatanga submarine valley. Filled paleoriver channels, identified in the Parasound profiles, suggest that the river runoff was continuous through four of the major valleys of the exposed Laptev Sea shelf during MIS 2. Similar LSR during the deposition of sediments characterized by the magnetic susceptibility peak and Holocene deposits imply an increased input of magnetic material during approximately 13.4–10 ka. This increased input is interpreted as a reflection of the deglaciation of the Anabar shield and the Putoran Plateau and the subsequent release of fine-grained glacial debris enriched in ferrimagnetic minerals into the Khatanga and Anabar rivers.

Acknowledgements We are indebted to the captain and crew of RV "Polarstern" and our fellow scientists for their help in collecting the data. We thank the members of the Geology Section of the Alfred Wegener Institute for constructive discussions, and C. Müller for correcting the manuscript. We thank the reviewers C.F. Forsberg and J. Mienert for valuable comments. This work was funded by the German Federal Ministry for Education, Research and Technology, BMBF-Forschungsverbund "ARKTIEF".

References

- Are FE (1994) Dynamics of the littoral zone of Arctic Seas (state of the art and goals). *Polarforschung* 64:123–131
- Arkhipov SA, Bespaly VG, Ehlers J, Johnson RG, Wright HE Jr (1995) Glacial drainage towards the Mediterranean during the Middle and Late Pleistocene. *Boreas* 24:196–206
- Bauch HA, Cremer H, Erlenkeuser H, Kassens H, Kunz-Pirring M (1996) Holocene paleoenvironmental evolution of the northern central Siberian shelf. In: *Quaternary Environment of the Eurasian North (QUEEN)*, First Annual Workshop, Strasbourg, France, Abstract Volume
- Behrends M (1999) Reconstructions of sea-ice drift and terrigenous sediment supply in the Late Quaternary: heavy-mineral associations in sediments of the Laptev-Sea continental margin and the Central Arctic Ocean. *Rep Polar Res* 310:167
- Benthien A (1994) Echographiekartierung und physikalische Eigenschaften der oberflächennahen Sedimente der Laptevsee. Thesis, Christian-Albrechts-Universität, Kiel, pp 80
- Blanchon P, Shaw J (1995) Reef drowning during the last deglaciation: evidence for catastrophic sea-level rise and ice-sheet collapse. *Geology* 23:4–8
- Chang S-BR, Kirschvink JL (1989) Magnetofossils, the magnetization of sediments and the evolution of magnetite biomineralisation. *Ann Rev Earth Planet Sci* 17:169–195
- Damuth JE (1975) Echo character of the western equatorial Atlantic floor and its relationship to the dispersal and distribution of terrigenous sediments. *Mar Geol* 18:17–45
- Damuth JE (1980) Use of high-frequency (3.5–12 kHz) echograms in the study of near-bottom sedimentation processes in the deep-sea: a review. *Mar Geol* 38:51–75
- Dearing J (1994) Environmental magnetic susceptibility. Using the Bartington MS2 System. Chi Publishing, Kenilworth, UK, pp 104
- Duzhikov OA, Strunin BM (1992) Geological outline of the Noril'sk region. In: Duzhikov OA, Strunin BM (eds) *Geology and metallogeny of sulfide deposits. Noril'sk region. USSR SEG Spec Publ*, pp 1–60
- Emery D, Myers KJ (1996) *Sequence stratigraphy*. Blackwell, London
- Fairbanks RG (1989) A 17,000-year glacio-eustatic sea level record: influence of glacial melting rates on the Younger Dryas event and deep-ocean circulation. *Nature* 342:637–642
- Fujita K, Cook DB (1990) The Arctic continental margin of eastern Siberia. In: Grantz A, Johnson L, Sweeney JF (eds) *The Arctic Ocean region*. Geological Society of America, Boulder, Colorado, pp 289–305
- Fütterer DK (1994) The expedition ARCTIC'93, Leg ARK-IX/4 of RV "Polarstern" 1993. *Rep Polar Res* 149:244
- Gordienko PA, Laktionov AF (1969) Circulation and physics of the Arctic Basin waters. *Oceanography* 46:94–112
- Grant JA, Schreiber R (1990) Modern swath sounding and sub-bottom profiling technology for research applications: the Atlas Hydrosweep and Parasound systems. *Mar Geophys Res* 12:9–19
- Holmes ML, Creager JS (1974) Holocene history of the Laptev Sea continental shelf. In: Herman Y (eds) *Marine geology and oceanography of the Arctic seas*. Springer, Berlin Heidelberg New York, pp 211–230
- Jones EP, Rudels B, Anderson LG (1995) Deep waters of the Arctic Ocean: origins and circulation. *Deep-Sea Res* 42:737–760
- Kassens H, Karpuy VY (1994) Russian-German Cooperation: the Transdrift I Expedition to the Laptev Sea, pp 168
- Kleiber HP, Niessen F (1999) Late Pleistocene paleoriver channels on the Laptev Sea shelf: implications from sub-bottom profiling. In: Kassens H, Bauch HA, Dmitrenko I, Eicken H, Hubberten HW, Melles M, Thiede J, Timokhov L (eds) *Land-ocean systems in the Siberian Arctic: dynamics and history*. Springer, Berlin Heidelberg New York, pp 657–665
- Kleiber HP, Niessen F, Weiel D (in press) The Late Quaternary evolution of the western Laptev Sea continental margin, Central Siberia (Arctic Ocean): implications from sub-bottom profiling. *Global Planet Change Spec QUEEN issue*
- Knies J (1999) Late Quaternary paleoenvironment along the northern Barents and Kara seas continental margin. *Rep Polar Res* 304:159
- Kögler FC (1963) Das Kastenlot. *Meyiana* 13:1–7
- Melles M, Hahne J, Siegert C, Bolshiyakov YB (1996) The Taymar Project: first results concerning the late Quaternary climatic and environmental history of northern Central Siberia. In: *Quaternary environment of the Eurasian North (QUEEN)*, First Annual Workshop, Strasbourg, France, Abstract Volume

- Niessen F, Weiel D (1996) Distribution of magnetic susceptibility on the Eurasian shelf and continental slope: implications for source areas of magnetic minerals. In: Stein R, Ivanov GI, Levitan MA, Fahl K (eds) Surface-sediment composition and sedimentary processes in the central Arctic Ocean and along the Eurasian Continental Margin. *Rep Polar Res* 149:81–88
- Nørgaard-Pedersen N (1996) Late Quaternary Arctic Ocean sediment record: surface ocean conditions and provenance of ice-rafted debris. *GEOMAR Rep* 65:115
- Nürnberg D, Fütterer DK, Niessen F, Nørgaard-Pedersen N, Schubert CJ, Spielhagen RF, Wahsner M (1995) The depositional environment of the Laptev Sea continental margin: preliminary results from the R/V "Polarstern" ARK IX-4 cruise. *Polar Res* 14:43–53
- Peregovich B, Hoops E, Rachold V (1999) Sediment transport to the Laptev Sea (Siberian Arctic) during the Holocene: evidence from the heavy mineral composition of fluvial and marine sediments. *Boreas* 28:205–214
- Pratson LF, Laine EP (1989) The relative importance of gravity-induced versus current-controlled sedimentation during the Quaternary along the mid-east U.S. outer continental margin revealed by 3.5 kHz echo character. *Mar Geol* 89:87–126
- Rachold V, Eisenhauer A, Hubberten H-W, Meyer H (1997) Sr isotopic composition of suspended particulate material (SPM) of East Siberian rivers: sediment transport to the Arctic Ocean. *Arctic Alpine Res* 29:422–429
- Rachor E (1997) Scientific Cruise Report of the Arctic Expedition ARK-XI/1 of RV "Polarstern" in 1995. *Rep Polar Res* 226:157
- Rudels B, Jones EP, Anderson LG, Kattner G (1994) On the intermediate depth waters of the Arctic Ocean. In: Johannessen OM, Muench RD, Overland JE (eds) The polar oceans and their role in shaping the global environment: the Nansen centennial volume. American Geophysical Union, Washington, D.C., pp 33–46
- Shackleton NJ (1987) Oxygen isotopes, ice volumes and sea level. *Quaternary Sci Rev* 6:183–190
- Spielhagen RF, Erlenkeuser H, Heinemeier J (1996) Deglacial changes of freshwater export from the Laptev Sea to the Arctic Ocean. In: Quaternary environment of the Eurasian North (QUEEN), First Annual Workshop, Strasbourg, France, Abstract Volume
- Spiess V (1993) Digitale Sedimentechographie – Neue Wege zu einer hochauflösenden Akustostratigraphie. *Berichte FB Geowiss Univ Bremen* 35:199
- Stein R (1996) Organic-carbon and carbonate distribution in Eurasian continental margin and Arctic Ocean deep-sea surface sediments: sources and pathways. In: Stein R, Ivanov GI, Levitan MA, Fahl K (eds) Surface-sediment composition and sedimentary processes in the central Arctic Ocean and along the Eurasian Continental Margin. *Rep Polar Res* 149:243–267
- Stein R, Fahl K (2000) Holocene accumulation of organic carbon at the Laptev Sea Continental Margin (Arctic Ocean): sources, pathways, and sinks. *GeoMarine Lett* 20:27–36
- Stein R, Korolev S (1994) Shelf-to-basin sediment transport in the eastern Arctic Ocean. In: Kassens H, Hubberten HW, Pryamikov, Stein R (eds) Russian–German cooperation in the Siberian shelf seas: geo-system Laptev Sea. *Rep Polar Res* 144:87–100
- Stein R, Fahl K, Niessen F, Siebold M (1999) Late Quaternary organic carbon and biomarkers records from the Laptev Sea Continental margin (Arctic Ocean): implications for organic carbon flux and composition. In: Kassens H, Bauch HA, Dmitrenko I, Eicken H, Hubberten HW, Melles M, Thiede J, Timokhov L (eds) Land-ocean systems in the Siberian Arctic: Dynamics and History. Springer-Verlag, Berlin, pp 633–655
- Stein R, Boucsein B, Fahl K, Garcia de Oteyza T, Knies J, Niessen F (in press) Accumulation of particulate organic carbon at the Eurasian continental margin during late Quaternary times: controlling mechanisms and paleoenvironmental significance. *Global Planet Change Spec QUEEN* issue
- Suslov SP (1961) Physical geography of the Asiatic Russia. Freeman, San Francisco
- Svendsen JI, Astakov VI, Bolshiyarov DY, Demidov I, Dowdeswell JA, Gataullin V, Hjort C, Hubberten HW, Larsen E, Mangerud J, Melles M, Möller P, Saarnisto M, Siegert MJ (1999) Maximum extent of the Eurasian ice sheet in the Barents and Kara Sea region during the Weichselian. *Boreas* 28:234–242
- Thompson R, Oldfield F (1986) Environmental magnetism. Allen and Unwin, London
- Velichko AA, Isayeva LL, Makeyev VM, Matishov GG, Faus-tova MA (1997) Late Pleistocene glaciation of the Arctic shelf, and the reconstruction of the Eurasian ice sheet. In: Velichko AA (ed) Late Quaternary environments of the Soviet Union. University of Minnesota Press, Minneapolis
- Vinogradov VA, Gramberg IS, Pogrebitsky YE, Rabkin MI, Ravich MG, Sokolov VN, Sorokov DS (1973) Main features of geologic structure and history of North-Central Siberia. In: Pitcher MG (ed) Arctic Ocean. The American Association of Petroleum Geologists, Tulsa, Oklahoma
- Wahsner M, Müller C, Stein R, Ivanov G, Levitan M, Shelekhova E, Tarasov G (1999) Clay-mineral distribution in surface sediments of the Eurasian Arctic Ocean and continental margin as indicator for source areas and transport pathways: a synthesis. *Boreas* 28:215–233
- Weiel D (1997) Paläozeanographische Untersuchungen in der Vilkitsky-Strasse und östlich von Severnaya Zembla mit sedimentologischen und geophysikalischen Methoden. Thesis, University of Cologne, 138 pp